11th International Symposium on Turbulence and Shear Flow Phenomena (TSFP11)
Southampton, UK, July 30 to August 2, 2019

CHARACTERIZING INFLUENTIAL NETWORKED STRUCTURES IN ISOTROPIC TURBULENCE

Muralikrishnan Gopalakrishnan Meena & Kunihiko Taira
Mechanical and Aerospace Engineering, University of California, Los Angeles, CA 90095, USA
Mechanical Engineering, Florida State University, Tallahassee, FL 32310, USA
muraligm@ucla.edu, ktaira@seas.ucla.edu

ABSTRACT

We characterize the complex nonlinear vortical interactions in two- and three-dimensional decaying isotropic turbulence through network-theoretic formulations and use network-based measures to identify and quantify the effects of influential structures on mixing enhancement. The web of interactions among vortical elements can be represented in a network-based framework where the vortical elements are the nodes and the vortical interactions are edges quantified by induced velocity following the Biot-Savart law. We find relationship between enstrophy and interaction strength, distribution of which gives an overall interaction behavior of the flow. Identification of vortical communities, groups of closely interacting nodes, enables the classification of shear layers and vortex core dominated structures as network connector and peripheral structures respectively. These respective elements exhibit inter-community and intra-community interactions. Furthermore, we find that perturbing the connectors and peripherals by adding and removing energy respectively can enhance mixing in both 2D and 3D decaying isotropic turbulence.

INTRODUCTION

Modifying the characteristics of turbulence is one of the most challenging problems in science due to its nonlinear and multiscale dynamics. Characterizing the behavior of turbulent flows is pertinent to modeling and controlling them, essential to various applications in modern science and technology (Brunton & Noack, 2015). The field of network science quantifies and reveals crucial interaction-based phenomena in a wide range of physical systems ranging from internet to neurons in brain (Newman, 2010). In this work, we use network-theoretic formulations to characterize vortical interactions in 2D and 3D decaying isotropic turbulence. We find a relationship between node interaction strength and enstrophy. Furthermore, network-based community detection tools are used to identify groups of closely connected vortical elements and classify them as connectors and peripherals based on how they interact with the overall flow field. This information is used to assess the influence of such structures towards enhancing turbulent mixing.

VORTEX INTERACTION NETWORK

A network or graph $\mathscr{G}$ consists of vertices or nodes $\mathscr{V}$ connected by edges or links $\mathscr{E}$ which may be weighted $\mathscr{W}$, giving a definition $\mathscr{G} = \mathscr{G}(\mathscr{V},\mathscr{E},\mathscr{W})$ for the network (Newman, 2010). The connectivity among the nodes can be mathematically represented by the adjacency matrix as

$$A_{ij} = w_{ji}, \tag{1}$$

where w_{ij} represents the weighted connection from node i to j. If the connection from j to i is the same, then the edge is said to be undirected, else, directed. We use this formulation to express the interactions among vortical elements in fluid flows.

We represent the vortical elements in a flow field as the nodes and the nonlinear web of interactions among them as the weighted edges of a network, namely the vortical interaction network. The influence of vortical elements on each other imparts induced velocity on them, which is governed by the Biot-Savart law. This makes the induced velocity an appropriate choice to quantify the interaction among vortical elements (Nair & Taira, 2015). The generalized Biot-Savart formula for an incompressible flow in n dimensions is given by

$$\mathbf{u}(\mathbf{r},t) = \frac{1}{2(n-1)\pi}\int_V \frac{\boldsymbol{\omega}(\mathbf{r},t)\times\mathbf{r}}{||\mathbf{r}||^n}\mathrm{d}V. \tag{2}$$

The interaction between two vortical elements i and j in two vortical structures is depicted in Fig. 1. The magnitude of velocity induced by element i on j can be generalized as

$$u_{i\to j} = \begin{cases} \frac{|\Gamma_i|}{2\pi||\mathbf{r}_j-\mathbf{r}_i||}, & n=2 \\ \left|\left| \frac{\Gamma_i \mathrm{d}l_i}{4\pi}\hat{\mathbf{e}}_{\omega_i} \times \frac{(\mathbf{r}_j-\mathbf{r}_i)}{||\mathbf{r}_j-\mathbf{r}_i||^3} \right|\right|, & n=3 \end{cases} \tag{3}$$

where $\Gamma = ||\boldsymbol{\omega}(\mathbf{r},t)||\mathrm{d}A$ and $\hat{\mathbf{e}}_\omega = \boldsymbol{\omega}(\mathbf{r},t)/||\boldsymbol{\omega}(\mathbf{r},t)||$ are respectively, the strength and direction of vorticity of a vortex element of area $\mathrm{d}A$ and width $\mathrm{d}l$ at position $\mathbf{r}$. The adjacency matrix for the vortical interaction network (Nair & Taira, 2015; Taira *et al.*, 2016) is defined by

$$w_{ji} = u_{i\to j}. \tag{4}$$

For a flow field with n grid points, $A \in \mathrm{R}^{n^2\times n^2}$. The above formulation gives weighted, unsigned, directed vortical interaction networks for 2D and 3D flows, applicable for both Eulerian and Lagrangian description of flow fields. The network-theoretic representation allows us to utilize various network-based measures to characterize the connectivity and geometric properties of the complex nonlinear vortical interactions.

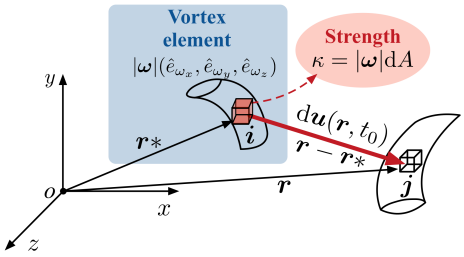

Figure 1. Interaction between two vortical elements.

Vortical interaction strength

The overall influence of a node in a network is given by the network strength of the node (Newman, 2010). The strength of each vortical node in a directed vortical network quantifies its ability to be influential (out-strength) or be influenced (in-strength) with respect to all the other nodes. The out- and in-strengths are given by

$$s_i^{out} = \sum_j A_{ij} \text{ and } s_i^{in} = \sum_j A_{ji}, \tag{5}$$

respectively. The present definition of the vortical network weight implicitly assumes the out-strength form. The probability distribution of strength $p(s)$ gives a global picture of the vortical network connectivity. The profile of the distribution is used to identify the type of the network, e.g., scale-free networks portraying a power-law distribution, $p(s) \sim s^{-\gamma}$ (Barabási, 2016).

For both 2D and 3D, the strength of an element i is

$$\Gamma_i = ||\boldsymbol{\omega}_i||\mathrm{d}A = \sqrt{\Omega_i}\mathrm{d}A, \tag{6}$$

where Ω_i is the enstrophy. The vortical node interaction strength can be reduced to,

$$s_i = \frac{\Gamma_i \mathrm{d}l}{2(n-1)\pi} f(\hat{\mathbf{e}}_{\omega_i}) \sum_j g(\Delta \boldsymbol{r}_{ij}) \tag{7}$$

$$= \frac{D}{2(n-1)\pi} \sqrt{\Omega_i} f(\hat{\mathbf{e}}_{\omega_i}) \mathrm{d}V \propto \sqrt{\Omega_i} f(\hat{\mathbf{e}}_{\omega_i}), \tag{8}$$

where the sum of distance components D is constant for all nodes. Thus, if the enstrophy distribution of a complex vortical flow follows a function $p(\Omega) = h(\Omega)$, which is usually known or can be obtained from observations for different fluid flow problems, then the strength distribution of the vortical flow network will also follow the function $h(s)$.

The above relations allows the network weight to be non-dimensionalized based on the enstrophy of the flow

$$\tilde{w}_{ij} = \begin{cases} \frac{w_{ij}}{A^{1/2}\Omega_{tot}^{1/2}} & \text{for 2D} \\ \frac{w_{ij}}{V^{1/3}\Omega_{tot}^{1/2}} & \text{for 3D,} \end{cases} \tag{9}$$

where Ω_{tot} is the total enstrophy of all the vortical elements per unit area or volume. The above non-dimensionalization allows us to analyze various types of vortical flow networks irrespective of the number of vortical elements due to varying resolution of the flow field representations, the total enstrophy differences based on the Re effects on different flow, and domain size.

Isotropic turbulence network

We analyze the network structure of 2D and 3D decaying isotropic turbulence using the above mentioned formulations and measures. A Fourier spectral (Taira *et al.*, 2016) and pseudo-spectral algorithm (Chumakov, 2008) is used to solve the Navier-Stokes equations in biperiodic and triperiodic domains for the 2D and 3D flows respectively. The network structure of the 2D decaying isotropic turbulence was analyzed by Taira *et al.* (2016) and have shown that the strength distribution follows a scale-free behavior as long as the energy spectrum follows the k^{-3} profile. For each of the flow mentioned, we use snapshots of vorticity data to construct the adjacency matrices. Regions with low values of $\|\boldsymbol{\omega}\|$ are removed. For the 2D dataset, subsampled flow fields from 1024×1024 to 128×128 are used for computing strength and other network measures discussed later. For 3D turbulence, we also use forced isotropic turbulence data from Johns Hopkins Turbulence Database Li *et al.* (2008). Subdomain (1/8th) of the $Re_\lambda = 418$ flow with a resolution of $1024 \times 1024 \times 1024$ is used for certain initial analyses. For further in-depth analyses, full periodic flow field of low Reynolds number cases with $Re_\lambda \in [30, 45]$ with a grid resolution of $64 \times 64 \times 64$ is computed through DNS.

The strength and enstrophy distributions of the vortical networks of 2D and 3D isotropic turbulence at an instant in time are shown in Fig. 2. We note that the enstrophy relations for network strength still holds. Benzi *et al.* (1987) have found power-law profile for the distribution of enstrophy for 2D decaying isotropic turbulence. The power-law distribution for the strength observed in Fig. 2 (top) is in conjecture with this observation as per our claim. For the three-dimensional turbulence, the enstrophy distribution follows a stretched-exponential profile (Donzis *et al.*, 2008), given by

$$P(\Omega) = g(\Omega) \sim \exp(-a_\Omega \Omega^b). \tag{10}$$

The distribution of s should also follow a similar function as $\Omega_i \approx s_i^2$. Thus, for 3D isotropic turbulence,

$$P(s^2) \approx g(s^2) \sim \exp(-a_s s^{2b}) \tag{11}$$

$$P(s) \sim \exp(-a_s s^b). \tag{12}$$

The stretched exponential distribution form of the out-strength with the same exponent as that of the enstrophy distribution is shown in Fig. 2 (bottom). The low-strength saturation from the power-law behavior of $P(s^2)$ in 2D corresponds to the presence of vortical elements with negligible strength. For 3D turbulence, the vorticity is spread over a wide scale of structures due to vortex stretching and tilting, which is absent in 2D flows. This corresponds to the absence of low-strength saturation in 3D and stretched exponential behavior of $P(s^2)$.

The node strength can be used to highlight the most influential vortical nodes in the flow field as shown in Fig. 3. Here, the network strength is visualized along with flow field measures of high positive Q-criterion and norm of strain tensor. The high network strength region aligns with both $Q > 0$ and $\|S\| > 0$. We ask the question of which structures in the flow field corresponds to the highly influential vortical structures in the flow. In an attempt to answer this question, we use community detection algorithm from network theory to identify these influential structures.

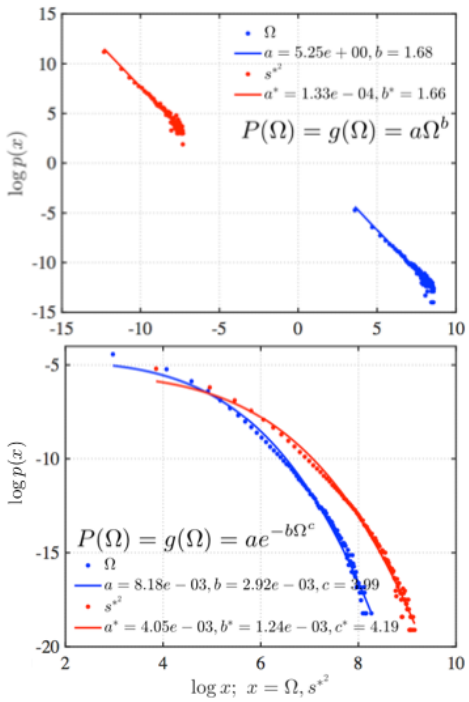

Figure 2. Enstrophy and network strength distributions of 2D (top) and 3D (bottom) isotropic turbulence.

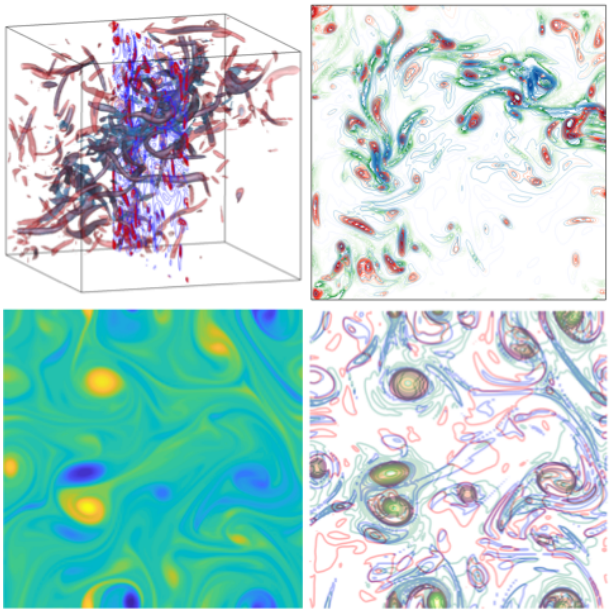

Figure 3. Comparing structures with high network strength s (blue), rotation Q (red), and strain $\|S\|$ (green) in a contour slice of a subdomain of high Re_λ 3D isotropic turbulence (top) and 2D isotropic turbulence (bottom).

VORTICAL COMMUNITIES

Identifying close connected vortical nodes is important towards revealing key coherent structures in a vortical flow. Such modular groups of nodes in a network with high connectivity amongst each other are called communities . The overall modular nature of the network structure is measured by modularity Q, given by (Leicht & Newman, 2008)

$$Q = \frac{1}{2n_e}\sum_{ij}\left[A_{ij} - \gamma_Q \frac{s_i^{\text{in}} s_j^{\text{out}}}{2n_e}\right]\delta(c_i, c_j), \tag{13}$$

where n_e is the total number of edges in the network, γ_Q is the modularity resolution parameter to weight the presence of small or large communities in the network, $\delta(i,j)$ is the Kronecker delta, $c_i \in \hat{C}_l$ is the label of the community to which element i is assigned and $\hat{C}_l$ is the set of l-th network community. Here, $l = 1, 2, \ldots, m$, with m being the total number of communities, unspecified and determined by the network-based algorithm. Identifying the communities involve regrouping the nodes so as to maximize modularity. Various algorithms are available to identify the communities in a network and we use the one developed by Blondel *et al.* (2008) to identify the communities in the vortical interaction network as shown for a sample case in Fig. 4 (a) (top). These communities represent vortical structures in a flow field containing vortical elements which interact closely and are specified as vortical communities (Gopalakrishnan Meena *et al.*, 2018).

The identification of vortical communities allows us to use various community-based network measures to analyze in-depth the connectivity within and amongst the communities, and hence, various vortical structures present in the flow field. The normalized z-score of the nodes within a community, called the within-module z-score (Guimera & Amaral, 2005), measures the intra-community interaction strength, how well a node is connected to other nodes in the same community, given by

$$z_{out_i} = \frac{\kappa_{i,i} - \overline{\kappa_{i,i}}}{\sigma_{\kappa_{i,i}}} \tag{14}$$

where $\kappa_{i,j} = \sum_{k \in C_j} A_{ik}$, $\overline{\kappa_{i,i}}$ is the average of κ over all the nodes in the community c_i, and $\sigma_{\kappa_{i,i}}$ is the standard deviation of κ in c_i. The inter-community interaction strength, ability of a node to interact with multiple communities measured by how well-distributed the links of a node is among different communities, is measured by the participation coefficient (Guimera & Amaral, 2005)

$$P_{out_i} = 1 - \sum_{k=1}^{m}\left(\frac{\kappa_{i,k}}{s_i}\right)^2. \tag{15}$$

If P is close to 1 then the links of node i are uniformly distributed among all communities and if it is 0 then the node is only connected to its own community. The $P-z$ map of nodes are important towards revealing key vortical elements within and among vortical communities. The $P-z$ map for the sample community detection results are shown in Fig.4 (a) (bottom). The nodes on the right side of the map will be well-connected ones, called the connectors, and the ones to the left side would be isolated groups, called peripherals. Also, top region with $z \gg 0$ consists of hub nodes and bottom region consists of weakly connected nodes. Through these network community-based formulations, the spatial distribution along with the strength of vortical structures are captured for extracting influential structures in the flow.

We do not observe a clear distinction between connectors and peripherals for the results depicted in Fig. 4 (a) (bottom). This is due to the vortical flow network being fully connected. The nodes with high vorticity strength are

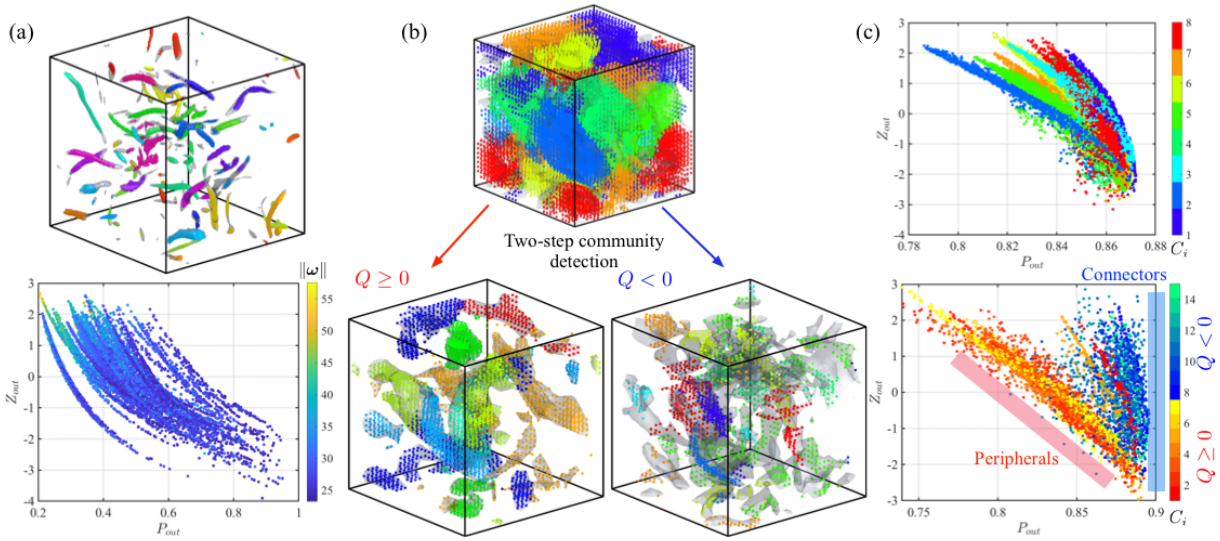

Figure 4. (a) Sample vortical community detection and corresponding $P-z$ map. (b) Two-step community detection and (c) corresponding $P-z$ maps.

highlighted as hubs. Also, the sample flow field is vorticity thresholded significantly to clearly depict the identification of coherent vortical communities. We implement the methodology to a full flow field of relatively low Re_λ as shown in Fig. 4 (b). Here, the initial community detection procedure coarsely identifies regions in the flow field with no distinct coherency and the $P-z$ map does not show clear distinction between connectors and peripherals.

With the assumption that highly rotational vortical elements and strained elements are ought to interact distinctly, we aid the community detection algorithm by splitting the flow field into two, one with nodes having $Q > 0$ and the other with $Q < 0$. We recompute the communities independently for these two sub-networks with initial guess from the previous step. The $P-z$ map is recomputed by combining the community information from these for the original full network. This two-step community detection procedure reveals the nodes to follow broadly two forms of correlations in the $P-z$ map. One set of nodes are oriented at a negative angle positioned on left side and the other oriented vertically on right side, and we classify them as peripheral and connector nodes respectively. The first group predominantly contains nodes with $Q > 0$ and the other with $Q < 0$. Most shear-layers are connector communities and vortex cores are peripheral communities. We observe similar result for 2D isotropic turbulence and for an ensemble of cases at various Re_λ. Given the classification of vortical structures into connectors and peripherals, let us now analyze how this network definition relates to fluid flow.

COMMUNITY-BASED PERTURBATION

The connector communities in network science are the ones which spread information throughout the network, influencing majority of the network. In fluid flow, given an input perturbation on connector communities in terms of energy, the perturbation should influence the flow in an inter-community manner. If we introduce some level of vorticity or velocity field fluctuation on such nodes, these fluctuations should affect the vorticity or velocity fluctuations of the whole flow field more compared to perturbing the peripheral communities. The later should make the perturbed region more organized or highly disorganized based on the direction of input (can be visualized as adding a perturbation to the core of a vortex in the or opposite direction of its rotation). Since the vortical network formulation is kinematic, we should expect this phenomena at least in a short time interval. We will explore how these affects would affect the flow field asymptotically also. Fluctuations as such should enhance turbulent mixing.

We perform analyses by perturbing individual communities obtaining a localized perturbation. We choose communities which are clearly distinct in their classification as a connector or peripheral and neglect those communities in the middle region of the $P-z$ map where their classification is ambiguous. Several ensemble of cases with varying initial condition and Re_λ are considered for both 2D as well as 3D isotropic turbulence. The identified connector and peripheral communities are perturbed so that the perturbed velocity (or vorticity) field at initial condition is given by,

$$\tilde{\boldsymbol{u}}(\boldsymbol{x},t_0) = \boldsymbol{u}(\boldsymbol{x},t_0) + A\tilde{\boldsymbol{f}}(\boldsymbol{x}) \tag{16}$$

where

$$\boldsymbol{f}(\boldsymbol{x}) = \frac{\hat{\boldsymbol{e}}_u}{\sqrt{2\pi\sigma^2}} \sum_{i=1}^{n_p} \exp\left(\frac{-\|\boldsymbol{x}-\boldsymbol{x}_i^*\|^2}{2\sigma^2}\right), \tag{17}$$

where σ is area or volume of the vortical element (grid size), $\hat{\boldsymbol{e}}_u$ is the unit vector in the direction of $\boldsymbol{u}$, $\boldsymbol{x}^* \in \{\boldsymbol{x} : c(\boldsymbol{x}) \in \hat{C}_l\}$ are the locations of the perturbed nodes, $c(\boldsymbol{x})$ is the community index of the node at $\boldsymbol{x}$, l is the index of the perturbed community, and n_p is the number of elements in $\hat{C}_l$. $\boldsymbol{f}(\boldsymbol{x})$ is normalized such that $\int_V \|\tilde{\boldsymbol{f}}(\boldsymbol{x})\|^2 dV = 1$, so that amplitude A is computed for a given energy input ratio C as

$$C = \frac{\int_V \|\tilde{\boldsymbol{u}}(\boldsymbol{x},t_0) - \boldsymbol{u}(\boldsymbol{x},t_0)\|^2 dV}{\int_V \|\boldsymbol{u}(\boldsymbol{x},t_0)\|^2 dV}. \tag{18}$$

The flow is simulated from this initial condition to assess the influence of the perturbation.

To quantify the fluctuation of velocity or vorticity fields, we analyze different measures, namely the Taylor microscale λ, variance of magnitude of vorticity $\sigma^2_{|\omega|}$, and variance of concentration of a passive scalar ϕ in the flow field $\sigma^2_{|\phi|}$. We keep the μ_ϕ same as that of the fluid flow. The decrease in the variance measures, suggesting homogeneity of the measure throughout the flow field, is also used as a measure to quantify the mixing enhancement achieved through the fluctuations in the flow field properties. The ensemble results for the perturbations on 2D and 3D isotropic turbulence are shown in Figs. 5 and 6 respectively.

For the 2D results, we input a $C = \pm 0.05$ for all the initial conditions. At short time interval, λ compared to baseline shows much larger decrease using connector-based perturbations, signifying the increase in small scale fluctuations in the flow field as expected. Peripheral-based perturbations with negative energy input also decreases λ for higher Re_λ cases as adding velocity or vorticity in the opposite direction of a vortex core would lead to vortex breakdown and hence decreasing the small scale lengths. The changes in $\sigma^2_{|\phi|}$ with respect to baseline case is insignificant over short time horizon as the mixing phenomena takes at least 1-2 eddy turnover time to prevail. The fluctuations in the vorticity magnitude measured by $\sigma^2_{|\omega|}$ are consistent with the changes in λ.

At longer time horizon, where mixing prevails, $\sigma^2_{|\omega|}$ decreases more for connector-based perturbations with $C = 0.05$ and *vice versa* for $C = -0.05$. This suggests enhanced vorticity distribution can be achieved through connector-based (shear layers) and peripheral-based (vortex cores) perturbations by adding and removing energy respectively. Although, the values of $\sigma^2_{|\phi|}$ are lower for peripheral-based perturbation for $C = \pm 0.05$ suggesting enhanced mixing. We will analyze the flow fields to better understand these variation between results of $\sigma^2_{|\omega|}$ and $\sigma^2_{|\phi|}$. Changes in the results of low *Re* cases are not significant to distinguish between connector and peripheral based perturbations.

For the 3D results, we only analyze the effects on λ and $\sigma^2_{|\omega|}$. We use an input of $C = \pm 0.1$ and yet there is no distinguishable trend in the results for connector and peripheral-based perturbations. We compare the qualitative results of 2D and 3D. The short time horizon results of 3D (at $Re_\lambda \in [30, 45]$) is similar to the low *Re* cases of 2D. Also, in long time horizon, the changes in λ are qualitatively similar to that observed in 2D. The results of $\sigma^2_{|\omega|}$ follow the same trend as in 2D. These suggests that we need to implement the perturbations for 3D in much higher *Re* cases. Implementing the passive scalar transport for the 3D cases would also help understand the phenomena better. These are part of the active ongoing work.

Using the inferences from the scalar measurements, we analyze the flow field evolution of a sample case in 2D with $C = 0.05$, portrayed in Fig. 7. The initial two snapshots at $t/\tau_{e_0} = t_1$ and t_2, where τ_{e_0} is the initial eddy turnover time of the baseline, shows the effect of the perturbations at short time horizon. The connector perturbations, applied on the shearlayer region, accelerates the shearlayer and rolls-up into smaller vortices (shortly after t_1 and is visible at t_2). These interact with nearby large vortices and modifies the flow, increasing the fluctuations of vorticity. The peripheral-based perturbation, applied on a vortex, increases the strength of the vortex and nearby region (t_1) and makes the structures more organized (t_2). These time horizons correspond to where decrease in λ are achieved more by connector-based perturbation. At long time horizon (t_3), the flow fields are significantly modified, as expected, with connector-based perturbation resulting in more smaller scale vortices and decreasing $\sigma^2_{|\omega|}$. Although, the values of $\sigma^2_{|\phi|}$ are comparatively larger for connector-based perturbation. The passive scalar concentration at this time instant t_3 is shown in Fig. 8. The results show that ϕ is larger at the region of smaller vortices and lower where strong vortices are located, maybe resulting from the choice of μ_ϕ. This decreases $\sigma^2_{|\phi|}$ when the flow field comprises of larger vortices as observed for peripheral-based perturbation. These observations from the flow field visualization further signifies the conclusion that shear layers and vortex cores can be used to enhance mixing in 2D decaying isotropic turbulence by adding and removing energy from them respectively.

CONCLUDING REMARKS

We use network-theoretic formulations to represent and quantify the vortical interactions in 2D and 3D decaying isotropic turbulence as a vortical network. We derive that network-based measure of node interaction strength is related to enstrophy. Furthermore, influential networked structures in the vortical network are extracted by identifying communities, groups of closely interacting elements in a network, and classifying them as connectors and peripherals using community-based measures of within-module z-score and participation coefficient. Connector nodes are those which interact with most communities and peripherals, ones which interact closely within their community. The spatial distribution along with the strength of vortical structures are incorporated through these network community-based formulations while identifying influential structures. Our results suggest that in isotropic turbulence, predominantly shear layers are the connectors whereas vortex cores are peripherals. Using this classification of vortical structures in the flow field, we perform community-based perturbation of connectors and peripherals and analyze the effect of such structures on the flow field. We find that shear layers and vortex cores can be used to enhance mixing in decaying isotropic turbulence by adding or removing energy from them respectively. For 3D results, there are ongoing efforts to examine such forms of perturbations at higher Reynolds numbers.

ACKNOWLEDGEMENT

The authors thank the US Army Research Office (Grant: W911NF-17-1-0118, Program Manager: Dr. Matthew Munson) for supporting this work. MGM also acknowledges the thought provoking discussions with James C. McWilliams, Steven L. Brunton, Chi-An Yeh, and Aditya Nair.

REFERENCES

Barabási, A.-L. 2016 *Network Science*. Cambridge University Press.

Benzi, R, Patarnello, S & Santangelo, P 1987 On the statistical properties of two-dimensional decaying turbulence. *EPL (Europhysics Letters)* **3** (7), 811.

Blondel, Vincent D, Guillaume, Jean-Loup, Lambiotte, Renaud & Lefebvre, Etienne 2008 Fast unfolding of communities in large networks. *Journal of Statistical Mechanics: Theory and Experiment* **2008** (10), P10008.

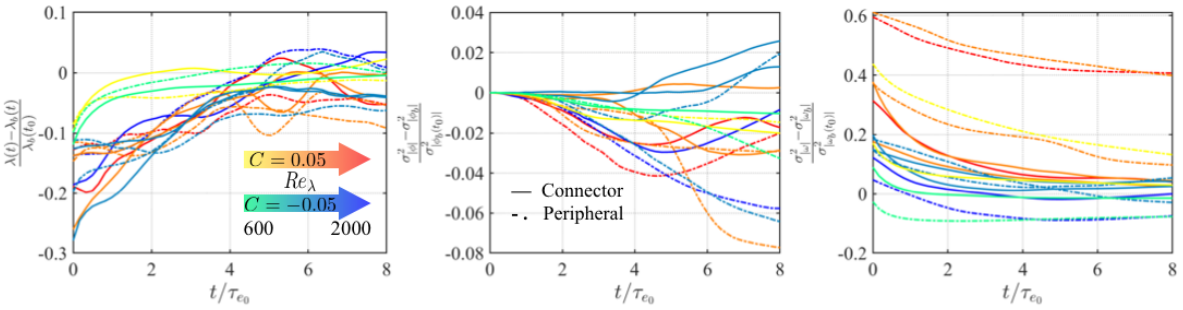

Figure 5. Results of community-based perturbation of 2D isotropic turbulence.

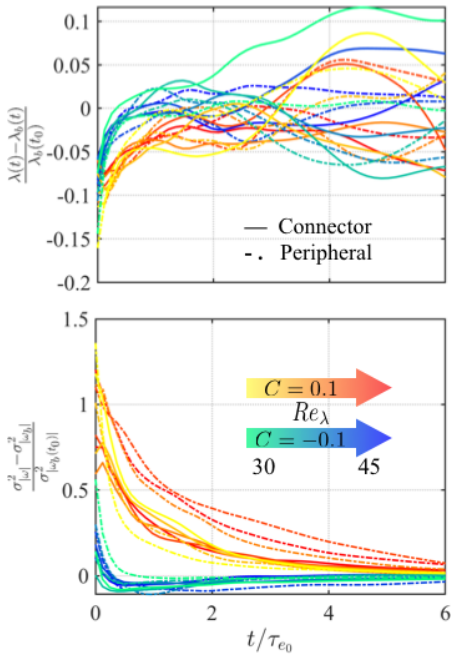

Figure 6. Results of community-based perturbation of 3D isotropic turbulence.

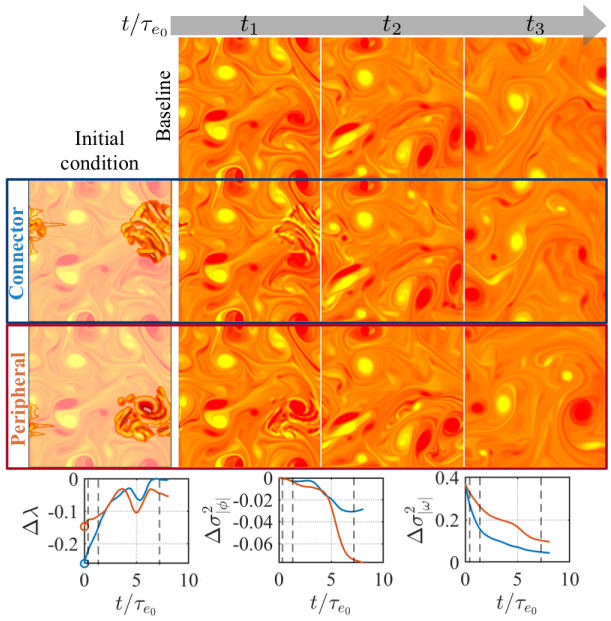

Figure 7. Snapshots of vorticity field evolution for localized connector (blue lines) and peripheral (red lines) perturbation in 2D turbulence for positive $C = 0.05$ at various time instants.

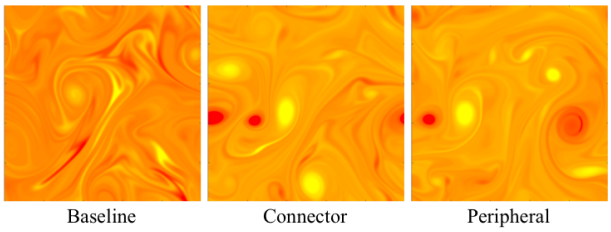

Figure 8. Snapshots of passive scalar concentration for perturbation in 2D turbulence for $C = 0.05$ at time t_3.

Brunton, Steven L & Noack, Bernd R 2015 Closed-loop turbulence control: progress and challenges. *Applied Mechanics Reviews* **67** (5), 050801.

Chumakov, Sergei G 2008 A priori study of subgrid-scale flux of a passive scalar in isotropic homogeneous turbulence. *Physical Review E* **78** (3), 036313.

Donzis, DA, Yeung, PK & Sreenivasan, KR 2008 Dissipation and enstrophy in isotropic turbulence: resolution effects and scaling in direct numerical simulations. *Physics of Fluids* **20** (4), 045108.

Gopalakrishnan Meena, Muralikrishnan, Nair, Aditya G. & Taira, Kunihiko 2018 Network community-based model reduction for vortical flows. *Phys. Rev. E* **97**, 063103.

Guimera, Roger & Amaral, Luis A Nunes 2005 Functional cartography of complex metabolic networks. *nature* **433** (7028), 895.

Leicht, Elizabeth A & Newman, Mark E J 2008 Community structure in directed networks. *Physical Review Letters* **100** (11), 118703.

Li, Yi, Perlman, Eric, Wan, Minping, Yang, Yunke, Meneveau, Charles, Burns, Randal, Chen, Shiyi, Szalay, Alexander & Eyink, Gregory 2008 A public turbulence database cluster and applications to study lagrangian evolution of velocity increments in turbulence. *Journal of Turbulence* (9), N31.

Nair, Aditya G & Taira, Kunihiko 2015 Network-theoretic approach to sparsified discrete vortex dynamics. *Journal of Fluid Mechanics* **768**, 549–571.

Newman, M. E. J. 2010 *Networks: an introduction*. Oxford Univ. Press.

Taira, Kunihiko, Nair, Aditya G & Brunton, Steven L 2016 Network structure of two-dimensional decaying isotropic turbulence. *Journal of Fluid Mechanics* **795**, R2.